

*Journal of*  
***Mechanics of***  
***Materials and Structures***

**ACTIVE CONTROL SCHEMES BASED ON THE LINEARIZED  
TSCHAUNER–HEMPEL EQUATIONS TO MAINTAIN THE  
SEPARATION DISTANCE CONSTRAINTS FOR THE NASA  
BENCHMARK TETRAHEDRON CONSTELLATION**

Pedro A. Capó-Lugo and Peter M. Bainum

*Volume 2, Nº 8*

*October 2007*



mathematical sciences publishers

# ACTIVE CONTROL SCHEMES BASED ON THE LINEARIZED TSCHAUNER–HEMPEL EQUATIONS TO MAINTAIN THE SEPARATION DISTANCE CONSTRAINTS FOR THE NASA BENCHMARK TETRAHEDRON CONSTELLATION

PEDRO A. CAPÓ-LUGO AND PETER M. BAINUM

The NASA benchmark tetrahedron constellation is a proposed satellite formation that requires a nominal separation distance at every apogee point. To maintain these separation distance constraints between any pair of satellites within the constellation, an open-loop scheme was developed based on the orbital elements. For a particular size of the NASA benchmark tetrahedron problem, the constellation maintains the separation distance conditions without perturbations. On the other hand, with perturbations, the constellation maintains the separation distance criteria for a limited number of orbits.

This scheme does not maintain the constellation together for the complete mission period. For this reason, the Tschauner–Hempel (TH) equations are used to maintain the separation distance criteria. Two control schemes are used to maintain the separation distance conditions of the tetrahedron constellation and are compared with each other to determine which one provides for minimum time and consumption.

## 1. Introduction

The proposed NASA benchmark tetrahedron constellation [Carpenter et al. 2003] is a complex problem because of the different strategies used to maintain the separation distance constraints. This benchmark problem is divided in three different specific sizes that contain different orbital dimensions for every orbit. For three specific sizes, we have analyzed the proposed constellation without the use of an active control scheme in which the strategy was based only on the orbital elements; for details see [Capó-Lugo 2005; Capó-Lugo and Bainum 2005b]. With this strategy the constellation satisfied the separation distance constraints for a short period of time without perturbations. When perturbations are added, the constellation violates the separation distance constraints in a limited number of complete orbits. After the first pair of satellites violates the separation distance conditions, an active control scheme is needed to maintain the separation distance criteria for an additional short period of time.

The motion of a pair of satellites around Earth is explained by the linearized Tschauner–Hempel (TH) equations. These equations describe the rendezvous of a pair of satellites in an elliptical orbit in which these satellites have a relative separation distance. To maintain the separation distance between a pair of satellites within the constellation, the linear quadratic regulator (LQR) is used as the active control scheme, but two different approaches are used with this active control scheme. Tan et al. [1999; 2002] and Bainum et al. [2004] (BST) developed an active control scheme which adapted in a piecewise manner the varying term in the linearized TH equations to correct the separation distance of an along-track

---

*Keywords:* tetrahedron constellation, linear quadratic regulator, elliptical orbits.

Research supported by the Alliances for Graduate Education and Professoriate (AGEP) Program.

constellation (or string of pearls). Carter and Humi [1987] and Carter [1990] (CH) developed a different control scheme based on the Pontryagin minimum principle, but a different formulation based on the CH approach is developed for the LQR control scheme. With these two techniques, one specific size of the NASA benchmark tetrahedron constellation is used to determine how the active control scheme is affected by these orbital dimensions and the different weighting matrices used in the LQR strategy. After the correction of the positions and velocities for a pair of satellites is performed, the Satellite Tool Kit [STK 2003] software is used to determine if the constellation is going to hold for another short period of time before a pair of satellites within the constellation violates the separation distance constraints. Hence, two active control schemes will be tested with one orbital size to understand their different responses to the correction of the separation distance between a pair of satellites.

## 2. Tetrahedron definition

The NASA benchmark tetrahedron configuration is similar to a pyramid, but the base of this configuration is an equilateral triangle with an apex point above the centroid of the triangle in a different plane [Carpenter et al. 2003; Capó-Lugo 2005; Capó-Lugo and Bainum 2005b]. Figure 1 shows the top and front view of the configuration. Points  $A$ ,  $B$ ,  $C$ , and  $H$  are the nominal positions of the satellites in the constellation, but throughout the paper these points will be also referred to as  $SA$ ,  $SB$ ,  $SC$ , and  $SH$ . Points  $B$  and  $C$  are nominally situated along the line of apsides, and points  $H$  and  $A$  are the satellites nominally orbiting around the centroid in a different orbital plane and in the equilateral triangle, respectively. The nominal separation distance between any two subsatellites at apogee is 10 km, and the separation error at subsequent apogees should be within 10%, giving an acceptable range between 9 and 11 km [Carpenter et al. 2003]. At other points in the orbit, the minimum separation distance between any pairs of subsatellites should be 1 km [Carpenter et al. 2003]. The purpose of this constellation is to measure the electromagnetic field of the Earth.

The positions of the satellites are determined from the reference point with respect to the Earth Coordinate Inertial (ECI) frame, given by point  $E$  in Figure 2. In this problem, the configuration is assumed such that the satellites arrive at the initial apogee point by some predetermined launch sequence. Figure 2 shows the tetrahedron configuration in the  $x$ - $y$  plane. This configuration is situated at the apogee point where  $r_a$  and  $r_p$  are the radii of apogee and perigee, respectively. As mentioned above,  $SB$  and  $SC$  are

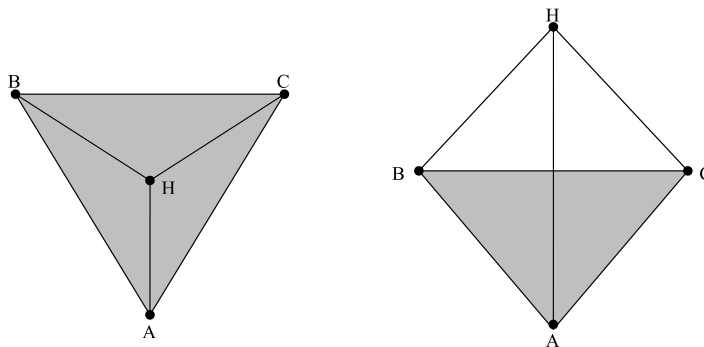


**Figure 1.** Top view (left side) and front view (right side) of the tetrahedron configuration.

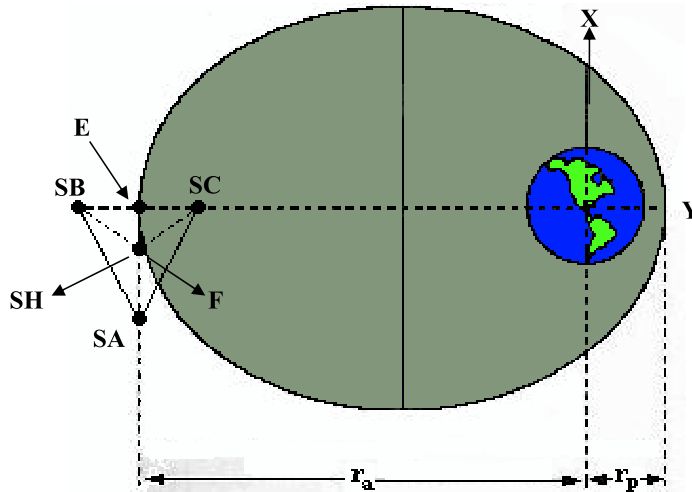


**Figure 2.** Two dimensional view of the configuration at apogee.

situated along the line of apsides ( $Y$  direction),  $SA$  forms the equilateral triangle, and  $SH$  is over the centroid in a different orbital plane. [Table 1](#) shows the initial positions of the constellation at the apogee point with respect to the ECI frame [[Capó-Lugo 2005](#); [Capó-Lugo and Bainum 2005b](#)].

### 3. Definition of the specific sizes (or phases)

The benchmark problem has four phases with a mission period of two years, but this research is only concerned with the three phases that contain the restrictions to maintain the separation distance constraints. [Table 2](#) details these three phases in terms of the orbital elements [[Carpenter et al. 2003](#); [Capó-Lugo 2005](#); [Capó-Lugo and Bainum 2005b](#)]. The fourth phase for the NASA benchmark problem is a lunar swing-by which is not considered here. [Table 2](#) shows the dimensions considered for the three phases.

The inclination angle in the third phase is not specified in the benchmark problem because the constellation must be in a near polar orbit, so this orbital inclination angle is chosen to be 85 degrees. As [Table 2](#) shows, the last phase has the largest orbit, smallest eccentricity and largest orbital period. Through this paper only phase I is analyzed with the LQR active control scheme.

Axis (ECI frame)	Ref. Point (km)	SA (km)	SB (km)	SC (km)	Centroid (km)	SH (km)
x	0	$-\overline{AE}$	0	0	$-\overline{EF}$	$-\overline{EF}$
y	$-r_a$	$-r_a$	$-(r_a + 5)$	$-(r_a - 5)$	$-r_a$	$-\frac{r_a}{2}$
z	0	0	0	0	0	$\frac{HF}{\sqrt{3}}$

**Table 1.** Initial satellite position at apogee with respect to the ECI frame, where  $\overline{AE} = 5\sqrt{3}$ ,  $\overline{EF} = 5/\sqrt{3}$ , and  $\overline{HF} = 10/\sqrt{3}$ .

Dimensions	First phase	Second phase	Third phase
Radius of perigee ( $r_p$ )	1.2 ER	1.2 ER	10 ER
Radius of apogee ( $r_a$ )	12 ER	30 ER	40 ER
Semimajor axis ( $a$ )	42,095.7 km	99,498.92 km	159,453.4 km
Eccentricity ( $e$ )	0.818	0.923	0.6
Inclination angle ( $i$ )	18.5°	18.5°	85.0°
Period (days)	1	2	7

**Table 2.** Dimensions and properties for the three phases; ER means Earth radius.

#### 4. Development of the equations of motion

The derivation of the equations of motion follows that of [Carter and Humi \[1987\]](#) who derived a set of equations to describe the rendezvous motion between a pair of satellites in an elliptical orbit for a general Keplerian orbit. For this application, the separation distance between a pair of satellites within the constellation is needed to be maintained at the apogee point to satisfy the separation distance constraints of the NASA benchmark problem [[Capó-Lugo and Bainum 2005b](#)].

The equations of motion are derived for a maneuvering satellite and a reference (target) satellite or point which is orbiting about the Earth in an elliptical orbit as shown in [Figure 3](#). The maneuvering satellite is assumed to have a scalar point mass  $m(t)$  and an applied thrust vector  $T(t)$  projected in the reference axis system. The target satellite is acted on by a Newtonian gravitational force directed toward the center of the Earth.  $R(t)$  is the vector measured from the center of the Earth to the reference or target satellite, and  $r(t)$  is the vector determined from the center of the Earth to the maneuvering satellite.  $\rho(t)$  (dashed line in [Figure 3](#)) is the vector measured from the reference satellite to the maneuvering satellite and describes their relative separation distance. The coordinate system is defined by two conditions. First,  $x_1$  is opposed to the motion of the maneuvering satellite and perpendicular to the  $x_2$ -axis, whose positive direction is along  $R(t)$ . Secondly,  $x_3$  is positive when the right handed system is completed.  $\omega$  is the relative angular velocity of the satellites about the Earth.

[Carter and Humi \[1987\]](#) developed a set of equations which explains the movement of a maneuvering spacecraft relative to the reference satellite in an elliptical orbit as shown in [Figure 3](#). This set of equations is dependent on the true anomaly angle  $\theta$  and is given by

$$(1 + e \cos \theta)x_1'' - (2e \sin \theta)x_1' = (e \cos \theta)x_1 - (2e \sin \theta)x_2 + 2(1 + e \cos \theta)x_2' + a_1, \tag{1}$$

$$(1 + e \cos \theta)x_2'' - (2e \sin \theta)x_2' = (2e \sin \theta)x_1 - 2(1 + e \cos \theta)x_1' + (3 + e \cos \theta)x_2 + a_2, \tag{2}$$

$$(1 + e \cos \theta)x_3'' - (2e \sin \theta)x_3' = -x_3 + a_3, \tag{3}$$

$$a_j = \frac{T_j}{m} \left( \frac{h^6}{\mu^4} \right) (1 + e \cos \theta)^{-3}, \quad \varphi' = \frac{d\varphi}{d\theta}, \quad \varphi'' = \frac{d^2\varphi}{d\theta^2},$$

where  $j = 1, 2, 3$  and  $\varphi$  is any function of the true anomaly angle. Equations (1)–(3) describe the Keplerian motion of the maneuvering satellite relative to the reference or target satellite for the special case where  $a_i$  (or  $T_i$ ) are zero. These equations can be solved analytically using transformations from

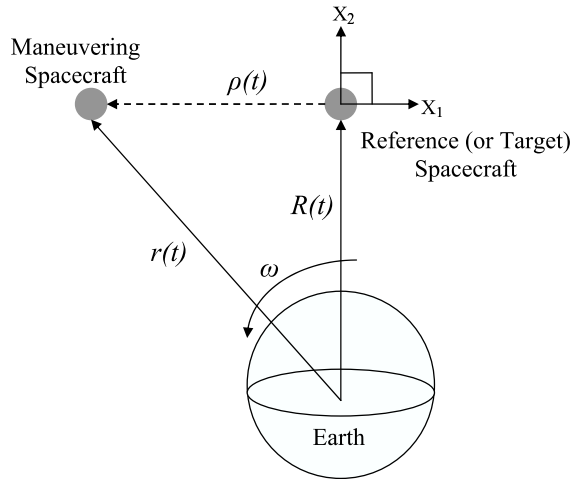


**Figure 3.** Reference and maneuvering satellite motion about Earth.

[Carter and Humi 1987]:

$$\{(1 + e \cos \theta)x_j\}' = (-e \sin \theta)x_j + (1 + e \cos \theta)x_j',$$

$$\frac{1}{1 + e \cos \theta} \{(1 + e \cos \theta)x_j'\}' = (1 + e \cos \theta)x_j'' - 2(e \sin \theta)x_j',$$

which then give

$$\frac{1}{1 + e \cos \theta} \{(1 + e \cos \theta)^2 x_1'\}' = (e \cos \theta)x_1 + 2\{(1 + e \cos \theta)x_2'\}' + a_1, \quad (4)$$

$$\frac{1}{1 + e \cos \theta} \{(1 + e \cos \theta)^2 x_2'\}' = (3 + e \cos \theta)x_2 - 2\{(1 + e \cos \theta)x_1'\}' + a_2, \quad (5)$$

$$\frac{1}{1 + e \cos \theta} \{(1 + e \cos \theta)^2 x_3'\}' = -x_3 + a_3. \quad (6)$$

Since

$$y_j = (1 + e \cos \theta)x_j, \quad y_j' = (1 + e \cos \theta)x_j' - (e \sin \theta)x_j,$$

and

$$y_j'' = (1 + e \cos \theta)x_j'' - (2e \sin \theta)x_j' - (e \cos \theta)x_j,$$

Equations (4)–(6) reduce to

$$y_1'' = 2y_2' + a_1, \quad y_2'' = 3\kappa y_2 - 2y_1' + a_2, \quad y_3'' = -y_3 + a_3, \quad (7)$$

where  $\kappa = \mu r/h^2 = 1/(1 + e \cos \theta)$  is determined from the well known equation of a Keplerian orbit (or equation of a conic section). Equations (7) are called the rendezvous linearized Tschauner–Hempel (TH) equations for the motion of a pair of satellites in an elliptical orbit. A control function  $u(t)$  can be used to represent the change in thrust  $T(\theta)$  and mass  $m(\theta)$  with respect to the true anomaly angle

[Carter and Humi 1987] via

$$\frac{T_m}{m_0} u_j(\theta) = \frac{T_j(\theta)}{m(\theta)}, \quad (8)$$

where  $T_m$  and  $m_0$  are the maximum thrust and initial mass of the maneuvering satellite. One can introduce new state variables  $\xi$ ,  $\zeta$ , and  $\eta$  by defining [Athans and Falb 1966]

$$v = \frac{h^6 T_m}{\mu^4 m_0}, \quad \xi = \frac{y_1}{v}, \quad \zeta = \frac{y_2}{v}, \quad \eta = \frac{y_3}{v}. \quad (9)$$

Using Equations (8) and (9), the linearized equations for the motion of the maneuvering satellite (see Equation (7)), in state-based format, can be expressed in the following form:

$$\begin{bmatrix} \xi' \\ \zeta' \\ \eta' \\ \xi'' \\ \zeta'' \\ \eta'' \end{bmatrix} = \begin{bmatrix} 0 & 0 & 0 & 1 & 0 & 0 \\ 0 & 0 & 0 & 0 & 1 & 0 \\ 0 & 0 & 0 & 0 & 0 & 1 \\ 0 & 0 & 0 & 0 & 2 & 0 \\ 0 & 3\kappa & 0 & -2 & 0 & 0 \\ 0 & 0 & -1 & 0 & 0 & 0 \end{bmatrix} \begin{bmatrix} \xi \\ \zeta \\ \eta \\ \xi' \\ \zeta' \\ \eta' \end{bmatrix} + \begin{bmatrix} 0 & 0 & 0 \\ 0 & 0 & 0 \\ 0 & 0 & 0 \\ \kappa^3 & 0 & 0 \\ 0 & \kappa^3 & 0 \\ 0 & 0 & \kappa^3 \end{bmatrix} \begin{bmatrix} u_1 \\ u_2 \\ u_3 \end{bmatrix}. \quad (10)$$

## 5. BST control approach

Tan et al. [1999; 2002] used the linearized TH equations to determine an active control scheme to satisfy the separation distance constraints for a constellation in an along-track formation (or string of pearls).

The active control scheme used by these authors is the linear quadratic regulator (LQR) which is an optimal control. To determine this active control law, they used the following quadratic cost function:

$$J = \frac{1}{2} \int_{\theta_0}^{\theta_f} \left\{ [(x(\theta) - x_D)^T Q (x(\theta) - x_D)] + [(u(\theta))^T R (u(\theta))] \right\} d\theta, \quad (11)$$

where  $x(\theta)$ ,  $x_D$  describes the components of the actual a desired state vector, respectively,  $u(\theta)$  is the control signal that will be used to maintain the separation distance constraints,  $Q$  and  $R$  are  $n \times n$  positive semidefinite and  $m \times m$  positive definite weight functioning matrices, respectively. This cost function is used to minimize the difference in the errors between the state vector and the desired state vector, and a minimum time problem can be obtained to maintain the separation distance criteria.

For these authors,  $\kappa = (\mu r)/h^2$ , and they adapt the nonlinear term in a piecewise manner. The nonlinear term in Equation (10) can be adjusted in a number of ways [Strong 2000; Bainum et al. 2004]:

1. When it is assumed that  $r$  remains constant, that is,  $r(\theta) = h^2/\mu$ , true for a circle and relatively short displacements, then, the term becomes 3.
2. If the simulation is started at perigee or apogee, then, evaluate  $r$  at perigee and apogee, respectively, and treat as constant for a sufficiently short time after.
3. If several orbits are needed to correct the disturbance, then, use an average value of  $r$  with  $h = rv = \sqrt{(b^2\mu)/a}$ , where  $b$  is the semiminor axis.
4. A final consideration is to update 1 and 2 in a piecewise adaptive manner along the orbit.

## 6. CH control approach

Carter and Humi [1987] and Carter [1990] used the same linearized TH equations, but with

$$\kappa = 1/(1 + e \cos \theta)$$

and with the control matrix  $B$  defined differently. BST assumed the  $B$  matrix as a control signal that produces some force to maintain the satellites in their corresponding relative distance between the reference (or target) and maneuvering satellite. For Carter and Humi, the  $A$  and  $B$  matrices vary with the true anomaly angle because Marec [1979] established that to obtain a minimum time problem with a minimum consumption of control the true anomaly must be considered as part of the controls for an elliptic orbit.

Carter and Humi used the Pontryagin minimum principle to obtain an admissible control such that the control scheme is used to rendezvous in an optimal way between the target satellite and the reference satellite [Carter and Humi 1987; Carter 1990]. Their cost function for the optimal control is given by

$$J = \int_{\theta_0}^{\theta_f} \frac{|u_i(\theta)|}{(1 + e \cos \theta)^2} d\theta. \quad (12)$$

Using this LQR strategy, let us define the cost function via the varying terms in the  $A$  and  $B$  matrices as

$$J = \frac{1}{2} \int_{\theta_0}^{\theta_f} \left\{ \frac{(x(\theta) - x_D)^T Q (x(\theta) - x_D)}{1 + e \cos \theta} + \frac{(u(\theta))^T R (u(\theta))}{(1 + e \cos \theta)^2} \right\} d\theta. \quad (13)$$

This proposed cost function is in accordance with Marec's statement for a minimum-time problem in an elliptical orbit and is based on the cost function defined by Carter and Humi.

## 7. Development of the linear quadratic regulator

Pontryagin minimum (or maximum) principles have been used by different authors to obtain an admissible control which leads to an optimal control that maintains the relative distance between the maneuvering and target satellite (or reference point) [Carter and Humi 1987; Carter 1990; Carter and Brient 1992; Massari et al. 2004]. Carter and Brient [1992] show that these principles apply to any elliptical orbit if the cost function is defined by Equation (13). On the other hand, a digital optimal control has been implemented by Massari et al. [2004] to maintain the orbit of some satellites in elliptical orbits, using the form of Equations (4)–(6), but their cost function is not defined in terms of the true anomaly angle. In this section, the linear quadratic regulator (LQR) technique will be developed to satisfy a minimum-time problem defined by the cost functions in Equations (11) and (13).

The LQR optimal control approach will be implemented with the use of the cost function defined by Equation (11). The solution of the LQR problem leads to an optimal feedback system with the property that the components of the state vector  $x(\theta)$  are kept near the desired state vector  $x_D$  without excessive expenditure of control energy [Athans and Falb 1966]. The existence of the optimal control is obtained from the solution of the Hamilton–Jacobi equation which is defined everywhere to obtain a minimum-time problem.

Consider the angle varying system defined by Equation (10) in the form

$$x' = Ax + Bu + \psi(\theta) \quad (14)$$

and the cost functional defined by Equation (11).  $\psi(\theta)$  is a  $n \times 1$  disturbance column matrix that can contain different perturbations such as the J2 (Earth's oblateness) perturbation, the drag force, Moon's gravity, and the solar pressure. It is defined as a function of the true anomaly angle. The  $A$  and  $B$  matrices have dimensions of  $n \times n$  and  $n \times m$ , respectively. It is assumed that for any initial state, there exists an optimal control which can obtain a desirable minimum consumption problem. The Hamiltonian  $H$  for the system in Equation (14) and the cost function in Equation (11) can be defined as

$$H = \frac{1}{2}|x(\theta) - x_D|^2 Q + \frac{1}{2}|u(\theta)|^2 R + A(\theta)x(\theta) \cdot p(\theta) + B(\theta)u(\theta) \cdot p(\theta) + \psi(\theta) \cdot p(\theta).$$

The minimum principles are used to obtain the necessary conditions for the optimal control [Athans and Falb 1966]. The costate vector  $p(\theta)$  is the solution of the vector differential equations

$$p'(\theta) = -\frac{\partial H}{\partial x(\theta)} = -Q(x(\theta) - x_D) - A^T(\theta)p(\theta). \quad (15)$$

The optimal trajectory is given by

$$\frac{\partial H}{\partial u(\theta)} = 0 = u(\theta)R + B^T(\theta)p(\theta), \quad u(\theta) = -R^{-1}B^T(\theta)p(\theta). \quad (16)$$

Using Equation (16), the angle varying differential equations defined by the Hamiltonian above can be rewritten as

$$x' = A(\theta)x - S(\theta)p(\theta) + \psi(\theta), \quad S(\theta) = B(\theta)R^{-1}B^T(\theta). \quad (17)$$

$S(\theta)$  is a square  $n \times n$  matrix. Using the transversality conditions defined in [Athans and Falb 1966] the costate variables have the following relationship,

$$p(\theta) = k(\theta)x(\theta) + m(\theta). \quad (18)$$

The  $k(\theta)$  and  $m(\theta)$  matrices are  $n \times n$  and  $n \times 1$ , respectively. They depend on the final angle  $\theta_f$  and a weighting matrix in the final state [Athans and Falb 1966], but not on the initial state. The solutions of the state and costate vectors are related by Equation (18). Upon differentiating it with respect to the true anomaly angle and substituted into Equation (15), the costate variables can be written as

$$k'(\theta)x(\theta) + k(\theta)x'(\theta) + m'(\theta) = -Qx(\theta) - A^T(\theta)p(\theta) + Qx_D.$$

Substituting Equation (17) into the above equation, we get

$$k'(\theta)x(\theta) + k(\theta)\{A(\theta)x(\theta) + S(\theta)(k(\theta)x(\theta) + m(\theta)) + \psi(\theta)\} + m'(\theta) = -Qx(\theta) - A^T(\theta)p(\theta) + Qx_D,$$

which can be separated into two equations

$$k'(\theta) = -A^T(\theta)k(\theta) - k(\theta)A(\theta) + k(\theta)S(\theta)k(\theta) - Q, \quad (19)$$

$$m'(\theta) = (k(\theta)S(\theta) - A^T(\theta))m(\theta) + Qx_D - k(\theta)\psi(\theta). \quad (20)$$

Equations (19) and (20) are the Ricatti equation (RE) and the adjoint Ricatti equation (ARE), respectively. The RE and ARE must be solved backwards in time as explained in [Phillips and Nagle 1995]. This system can be solved using Runge–Kutta methods, but, this method always runs forward in time. For this reason, Euler's method is used to obtain an approximate solution since it can be applied backwards in time [Strang 1986; Borse 2000; Gerald and Wheatley 2004]. Euler's method must be applied until a

stable solution is obtained, but, instead of using this method to obtain a stable solution for the RE and ARE, the system can be defined continuously with respect to the true anomaly angle. In this way, a solution is obtained in the stable region. The following approximation can be applied for the system

$$\lim_{\Delta\theta \rightarrow \infty} k'(\theta) = \lim_{\Delta\theta \rightarrow \infty} m'(\theta) = \lim_{\Delta\theta \rightarrow \infty} \frac{k(\theta + \Delta\theta) - k(\theta)}{\Delta\theta} = \lim_{\Delta\theta \rightarrow \infty} \frac{m(\theta + \Delta\theta) - m(\theta)}{\Delta\theta} = 0.$$

Equations (19) and (20) become

$$0 = -A^T(\theta)k(\theta) - k(\theta)A(\theta) + k(\theta)S(\theta)k(\theta) - Q, \quad (21)$$

$$m(\theta) = (A^T(\theta) + k(\theta)S(\theta))^{-1}(Qx_D - k(\theta)\psi(\theta)). \quad (22)$$

The state vector can be solved using a numerical integration scheme such as the Runge–Kutta method since this integration process runs forward in time. Substituting Equation (18) into Equation (17), the state vector is defined as  $x'(\theta) = A(\theta)x(\theta) - S(\theta)k(\theta)x(\theta) - S(\theta)m(\theta) + \psi(\theta)$ . With Equations (16) and (18), the control vector is  $u(\theta) = -S(\theta)(k(\theta)x(\theta) + m(\theta))$ .

The following procedure is adapted to obtain a solution for the RE, the ARE, the state vector, and the control vector:

1. Use Equations (21) and (22) to obtain a solution for the RE and the ARE.
2. Substitute these values for  $k(\theta)$  and  $m(\theta)$  (continuous in time) into the state vector equation, and integrate forward in time using any numerical scheme.
3. Substitute these values for  $k(\theta)$ ,  $m(\theta)$ , and  $x(\theta)$  to determine  $u(\theta)$ .

## 8. BST approach to the LQR active control scheme

The LQR is determined from the cost function defined by Equation (11). The  $Q$  and  $R$  matrices do not vary with the true anomaly angle. Then, the RE and the ARE are

$$0 = -A^T(\theta)k_\infty - k_\infty A(\theta) + k_\infty S(\theta)k_\infty - Q, \quad m_\infty = (A^T(\theta) + k_\infty S(\theta))^{-1}(Qx_D - k_\infty \psi(\theta)).$$

$k_\infty$  and  $m_\infty$  are constants if the matrix is completely controllable and continuous with respect to the true anomaly angle. The state vector equation and the control vector are then given by

$$x'(\theta) = A(\theta)x(\theta) - Sk_\infty x(\theta) - Sm_\infty + \psi(\theta), \quad u(\theta) = -S(k_\infty x(\theta) + m_\infty).$$

These substitutions are performed because the authors adapt in a piecewise manner the angle varying term in the  $A$  matrix which is going to be constant for short periods of time.

## 9. Carter–Humi approach to the LQR active control scheme

For this control scheme, the LQR is complex because the cost function defined by Equation (13) varies with the true anomaly angle and therefore takes the form of an elliptical integral. Define it by

$$J = \frac{1}{2} \int_{\theta_0}^{\theta_f} \{ (x(\theta) - x_D)^T \tilde{Q} (x(\theta) - x_D) + (u(\theta))^T \tilde{R} u(\theta) \} d\theta, \quad \tilde{Q} = \frac{Q}{1 + e \cos \theta}, \quad \tilde{R} = \frac{R}{(1 + e \cos \theta)^2}.$$

Then, the RE and ARE, continuous with respect to the true anomaly angle, are defined as

$$0 = -A^T(\theta)k(\theta) - k(\theta)A(\theta) + k(\theta)\tilde{S}(\theta)k(\theta) - \tilde{Q}, \quad m(\theta) = (A^T(\theta) + k(\theta)\tilde{S}(\theta))^{-1}(\tilde{Q}x_D - k(\theta)\psi(\theta)),$$

where  $\tilde{S}(\theta) = B(\theta)\tilde{R}^{-1}B^T(\theta)$ . These equations vary with the true anomaly angle instead of being constant for short periods of time as for BST. For the Carter–Humi control schemes, the differential equations are defined by Equation (10), where  $\kappa = 1/(1 + e \cos \theta)$ . The state and control vectors are

$$x'(\theta) = A(\theta)x(\theta) - \tilde{S}(\theta)k(\theta)x(\theta) - \tilde{S}(\theta)m(\theta) + \psi(\theta), \quad u(\theta) = -\tilde{S}(\theta)(k(\theta)x(\theta) + m(\theta)).$$

The same procedure to calculate the values for the RE, ARE, state vectors, and control vectors will be applied for this scheme, but the true anomaly angle will vary with the position of the satellites.

### 10. Reference and maneuvering satellite

The reference and maneuvering satellite must be chosen such that the linearized TH equations can be used to maintain the separation distance constraints [Capó-Lugo 2005; Capó-Lugo and Bainum 2005b; 2005a]. The maneuvering satellite is assumed to have an applied thrust along its reference axes to correct the separation distance with respect to the reference satellite. With only the Earth’s oblateness (J2) perturbation, the satellites near the centroid (SA-SH) maintain the separation distance constraints for a long period of time, but SA-SB and SA-SC violate the separation distance constraints in 6 complete orbits for phase I and must be corrected first as shown in [Capó-Lugo 2005; Capó-Lugo and Bainum 2005b]. Since SH-SA does not violate the separation distance constraints for a simulation time of 30 days, these two satellites are nominally on their orbits and can be used as references to correct the drift of the other two satellites, namely, SB and SC. For the in-plane motion, SA will be used as the reference satellite to correct the positions and velocities of the other two satellites along the semimajor axis, making SB and SC the maneuvering satellites. SH is not considered to correct its separation distance conditions, but it can be used to correct the out of plane motion of the other satellites.

The J2 perturbation has major effects on low-earth orbit (LEO) satellites, but, for this constellation, phase I is greatly disturbed at the perigee and apogee points because the altitude of the perigee point is very close to the Earth. This perturbation causes the constellation to violate the separation distance constraints in a limited number of complete orbits. Following [Mishne 2004] the J2 perturbation can be defined in component form as

$$\psi(\theta) = \begin{bmatrix} 0 \\ 0 \\ 0 \\ f_x \\ f_y \\ f_z \end{bmatrix} = \begin{bmatrix} 0 \\ 0 \\ 0 \\ -\frac{3}{2}J_2\frac{\mu}{r^2}\left(\frac{R_e}{r}\right)^2(1 - 3\sin^2 i \sin^2 \theta) \\ -3J_2\frac{\mu}{r^2}\left(\frac{R_e}{r}\right)^2(\sin^2 i \sin \theta \cos \theta) \\ -3J_2\frac{\mu}{r^2}\left(\frac{R_e}{r}\right)^2(\sin i \cos i \sin \theta) \end{bmatrix}, \quad (23)$$

where  $i$  is the inclination angle, and  $\theta$  is the true anomaly angle. For the NASA benchmark tetrahedron constellation, the inclination angle for phase I is equal to 18.5°. Equation (23) is the disturbance matrix defined in Equation (14) in terms of the true anomaly angle.

Nominal coordinates	Separation distance
$\xi_N = -8.6602543 \text{ km}$	$\xi_S = -9.928 \text{ km}$
$\zeta_N = 4.7416 \text{ km}$	$\zeta_S = 4.7 \text{ km}$
$\eta_N = 1.5865 \text{ km}$	$\eta_S = 1.5 \text{ km}$
$\xi'_N = 3.49665 \times 10^{-4} \text{ km/s}$	$\xi'_S = 3.51 \times 10^{-4} \text{ km/s}$
$\zeta'_N = 0 \text{ km/s}$	$\zeta'_S = -1.4 \times 10^{-5} \text{ km/s}$
$\eta'_N = 0 \text{ km/s}$	$\eta'_S = -9 \times 10^{-6} \text{ km/s}$

**Table 3.** Nominal coordinates and initial separation distance for SA-SB system in phase I.

To initialize the procedure to calculate the Riccati and adjoint Riccati equations, state variables, and the optimal control explained in the previous section, [Table 3](#) shows the nominal coordinates and the separation distance [[Capó-Lugo 2005](#); [Capó-Lugo and Bainum 2005b](#); [2005a](#)]. The first column illustrates the nominal separation distance coordinates for which the constellation satisfies the separation distance conditions at the apogee point. The second column shows the separation distance coordinates when the pair SA-SB first violates the separation distance criteria. These separation distances are obtained from [[Capó-Lugo 2005](#)] when the J2 perturbation is added into the STK simulations.

The relative drift from the reference satellite to the maneuvering satellite, in state-based variables  $(\xi, \zeta, \eta)$ , can be calculated as:

$$x(\theta_0) = \begin{bmatrix} \xi \\ \zeta \\ \eta \\ \xi' \\ \zeta' \\ \eta' \end{bmatrix} = \begin{bmatrix} \xi_S - \xi_N \\ \zeta_S - \zeta_N \\ \eta_S - \eta_N \\ \xi'_S - \xi'_N \\ \zeta'_S - \zeta'_N \\ \eta'_S - \eta'_N \end{bmatrix}. \quad (24)$$

[Equation \(24\)](#) represents initial conditions for system of differential equations defined by [Equation \(10\)](#), with the desired state vector  $x_D$  used in [Equations \(11\)](#) and [\(13\)](#) set equal to zero. With this scheme the satellites will reduce the relative drift in the separation distance and the velocity for a pair of satellites within the constellation such that, at the next apogee point, the satellites will satisfy the separation distance constraints.

## 11. Results of the active control laws

The two active control laws are studied to determine if there exists a difference between the methods to correct the drift between a pair of satellites. The main question is: how much weight do the  $Q$  and  $R$  matrices need? The  $Q$  and  $R$  matrices can have any values within the maximum limits on the magnitude of the control and can change the response in the system. Through these simulations, the matrices will be weighted in different ways.

Equations of motion are written in terms of the true anomaly angle, but the time that it takes to correct the drift between a pair of satellites can be determined with the following equations [[Massari et al. 2004](#)]:

$$\tan(E/2) = \sqrt{(1-e)/(1+e)} \tan(\theta/2), \quad n(t - t_\pi) = E - e \sin E, \quad (25)$$

where  $E$  is the eccentric anomaly,  $n$  is the mean motion of a satellite in which  $n = \sqrt{\mu/a^3}$ ,  $t_\pi$  is the time at the perigee point, and  $t$  is the time of the satellite at some point in the orbit. This transformation is used to determine how much time is required for the satellites to make the corrections. The time is changed from seconds to hours because the period of the orbit is expressed in days as shown in [Table 1](#), and a number of orbits can be obtained to understand when the maneuvering satellite finishes the corrections to the drift between a pair of satellites. The responses that will be obtained from the solution of the active control scheme will have particular units as follows: km for the correction in the separation distance, km/s for the velocity correction, and km/s<sup>2</sup> for the optimal control since it is expressed in terms of acceleration.

The optimal control  $u_j(\theta)$ , for  $j = 1, 2, 3$  also shows thrust levels because in [Equation \(10\)](#) the thrust  $T(\theta)$  is divided by the mass  $m(\theta)$  such that the terms can be expressed in terms of accelerations to develop the linearized TH equations. The directions of the axes in state variable format, defined by [Equation \(10\)](#), are as follows:  $\xi$  is positive against the motion of the spacecraft,  $\zeta$  is positive along the radial direction, and  $\eta$  is positive when the right hand system is completed. The thrust  $T(\theta)$  is specified in the same directions as  $\xi$ ,  $\zeta$ , and  $\eta$  in which the control function  $u(\theta)$  is defined over the same direction as the thrust  $T(\theta)$ .

The simulation begins at the apogee point where the constellation first violates the separation distance conditions and finishes at the following apogee point. Since the linear quadratic optimal controller is defined continuously in the true anomaly angle, the simulation can be expanded after one complete period, but, in some cases, the simulation time is shortened because, after the system of linear equations [\(10\)](#) comes into steady state, the same result is obtained through the complete simulation of the corresponding nonlinear equations. The Runge–Kutta method is used to integrate the linear equations forward in the true anomaly angle, where the step size is chosen to be 0.004 radians for this phase. This step size is small, but is used to diminish the error in the calculations. For the BST active control scheme, the  $\kappa$  term in [Equation \(10\)](#) is updated every 0.012 radians, but the active control scheme will depend mainly on the weighted matrices. In the simulations the following aliases are used: (1) xi  $\rightarrow$   $\xi$ , (2) zeta  $\rightarrow$   $\zeta$ , (3) eta  $\rightarrow$   $\eta$ , (4) Vxi  $\rightarrow$   $\xi'$ , (5) Vzeta  $\rightarrow$   $\zeta'$ , (6) Veta  $\rightarrow$   $\eta'$ , and (7)  $U1$ ,  $U2$ , and  $U3$  is the control vector in the directions of  $\xi$ ,  $\zeta$ , and  $\eta$  defined in [Equation \(10\)](#), respectively. This representation is used in the legend of all the simulations performed in this study.

The first set of initial conditions defined in [Table 3](#) are used to determine the drift between the position and velocity of SA and SB using [Equation \(24\)](#). [Table 2](#) details the values for the orbital elements defined in the state matrix  $A$ , the control matrix  $B$ , and [Equation \(25\)](#). The simulations are run with the BST active control scheme, and thereafter the Carter–Humi control scheme is implemented to compare the two different control techniques for the correction of the separation distance and velocity of a pair of satellites.

When  $Q = \text{diag}[20 \ 20 \ 20 \ 20 \ 20 \ 20]$  and  $R = \text{diag}[10 \ 10 \ 10]$  [Figure 4](#) shows the results with the BST and CH active control schemes. The correction in the separation distance and the velocity of the maneuvering spacecraft shows that the system is stabilized in approximately 5 hr, but, for the CH active control scheme, the optimal control effort is less than in the BST active control scheme. The cost function

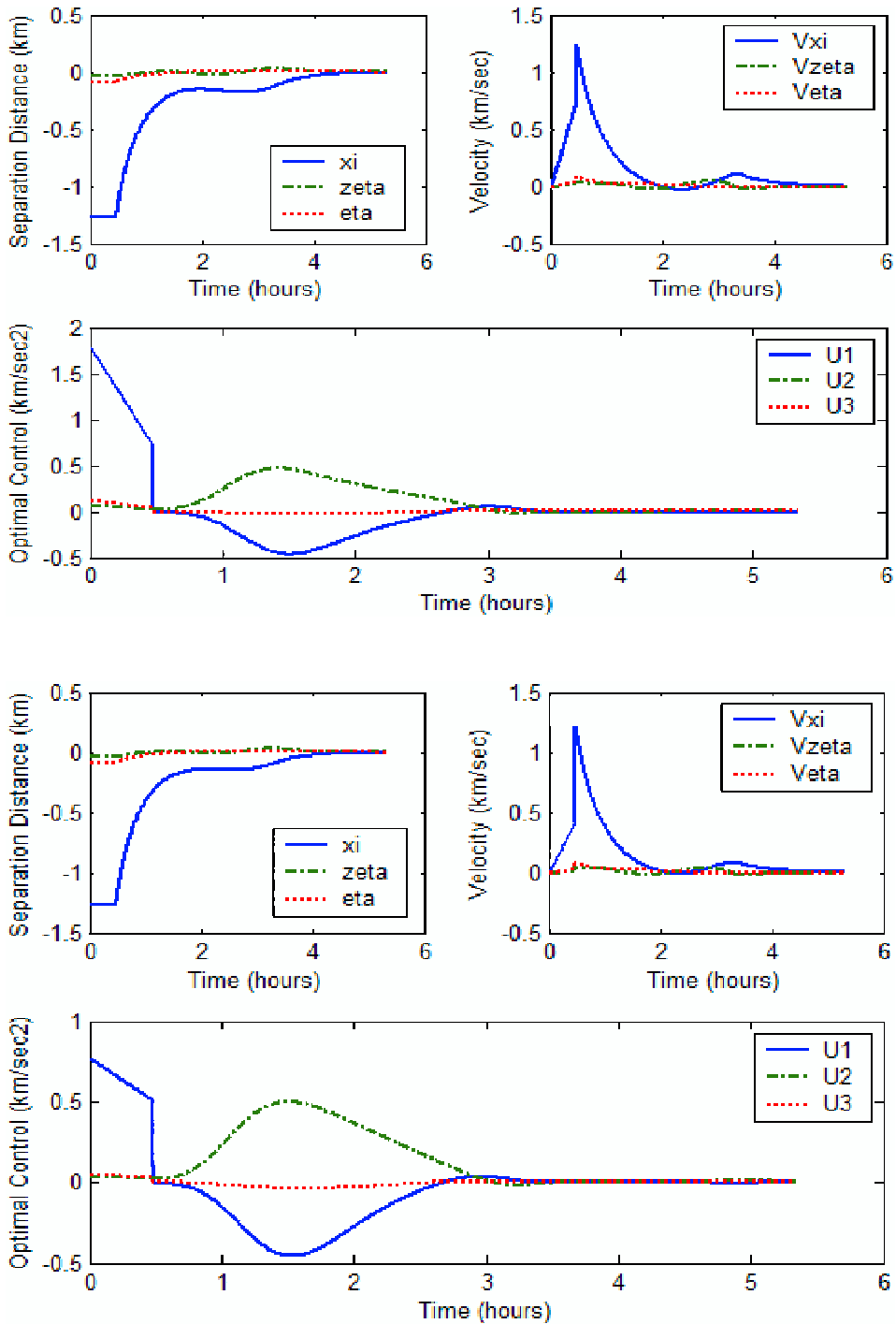


**Figure 4.** SA-SB separation distance correction using BST (top) and CH (bottom) active control scheme for  $Q = \text{diag}[20 \ 20 \ 20 \ 20 \ 20 \ 20]$  and  $R = \text{diag}[10 \ 10 \ 10]$ .

in the CH active control scheme varies with the true anomaly angle and uses the eccentricity term such that a minimum time and consumption problem can be obtained along the orbit.

If the  $Q$  matrix is split to weight the velocities  $\xi'$ ,  $\zeta'$ ,  $\eta'$  more than the positions  $\xi$ ,  $\zeta$ ,  $\eta$  while setting  $R = \text{diag}[20 \ 20 \ 20]$ , Figure 5 shows the results for the correction of the drift in the separation distance and velocities. In Figure 5 both control schemes show that the correction is going to take more time before a steady state response is obtained. In the BST active control scheme, the optimal control is going to be stabilized before 6 hr. In the CH active control scheme, the optimal control is stabilized after 8 hr, and the optimal control and the correction of the velocity shows lower levels than in the BST active control scheme. For the BST active control scheme, this weighting in the  $Q$  matrix will cause greater fuel expenditure, an undesired situation.

When the positions  $\xi$ ,  $\zeta$ ,  $\eta$  are weighted more than the velocities  $\xi'$ ,  $\zeta'$ ,  $\eta'$  Figure 6 shows the responses in the correction of the separation distance and velocity for the maneuvering spacecraft for both active control schemes. The weights for this case are  $Q = \text{diag}[20 \ 20 \ 20 \ 1 \ 1 \ 1]$  and  $R = \text{diag}[20 \ 20 \ 20]$ . For both active control schemes, the separation distance and the velocities are corrected faster compared to the previous case. The correction takes less than 2 hr for both active control schemes, but the CH active control schemes shows a lower level in the optimal control as well in the velocity.

Analyzing Equation (10), one sees that if the varying term in the  $A$  matrix is weighted more, then the active control scheme is going to take less time to stabilize the system; this is shown in Figure 6. On the other hand, when the velocities are weighted more, the system is going to take more time to stabilize the varying term; this is illustrated in Figure 5.

## 12. Examination of the drifts after the first correction

When the satellites move to the apogee point the constellation will satisfy the separation distance constraints, but the perturbations will still be present, and the constellation may hold for only a limited number of complete orbits. This situation may guarantee that the constellation will not violate the separation distance constraint at the following apogee point. The Satellite Tool Kit software [STK 2003] (STK) is used to propagate the constellation motion after the active control scheme has corrected the drift between a pair of satellites; in the last simulations, the correction in the drift of the separation distance is between SA and SC [Carpenter et al. 2003; Capó-Lugo 2005; Capó-Lugo and Bainum 2005b]. This pair of satellites violates the NASA benchmark tetrahedron conditions first. The STK motion is propagated from the apogee point after the correction is made, assuming that the satellites corrected the drift made by the J2 perturbation.

For phase I, Table 4 shows the initial conditions at the initial apogee point for the NASA benchmark tetrahedron constellation. The simulation for the correction in the positions and velocities between a pair of satellites for the BST and Carter–Humi active control schemes shows that the correction in the drift is less than  $1 \times 10^{-6}$  km for the separation distance and  $1 \times 10^{-6}$  km/sec for the velocities when the control schemes finish the correction. To start the simulation at the next apogee point, the drift is assumed to be  $1 \times 10^{-6}$  for the correction in the positions (km) and velocities (km/sec) between a pair of satellites after the correction is performed. This value is used because, if the correction for the J2 perturbation is made, the maneuvering satellites (SB and SC) satisfy the separation distance requirements at the following apogee point. This small drift is added into the initial conditions shown in Table 4 to determine if the

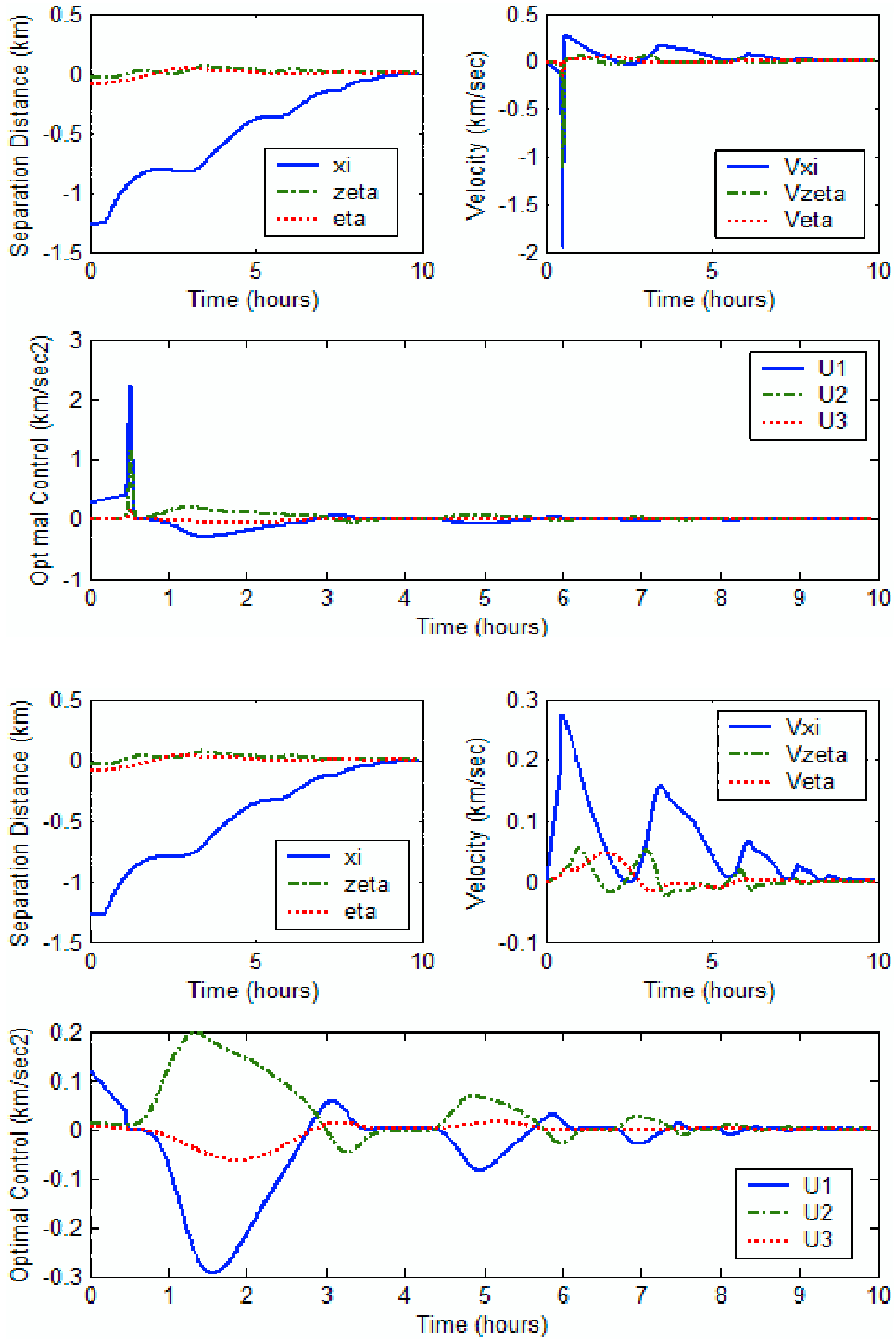


**Figure 5.** SA-SB separation distance correction using BST (top) and CH (bottom) active control scheme for  $Q = \text{diag}[1 \ 1 \ 1 \ 20 \ 20 \ 20]$  and  $R = \text{diag}[20 \ 20 \ 20]$ .

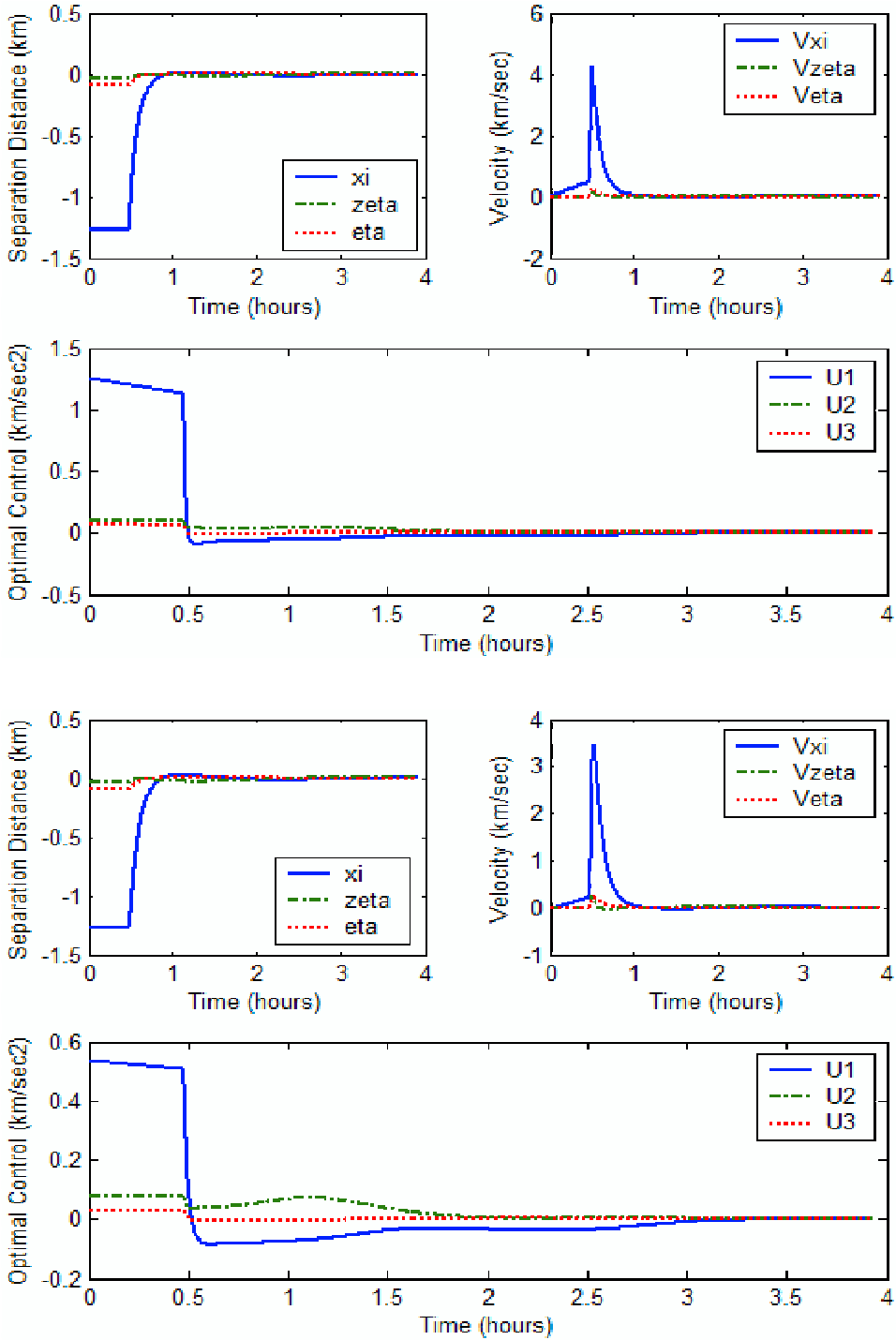


**Figure 6.** SA-SB separation distance correction using BST (top) and CH (bottom) active control scheme for  $Q = \text{diag}[20 \ 20 \ 20 \ 1 \ 1 \ 1]$  and  $R = \text{diag}[20 \ 20 \ 20]$ .

Satellite	$x$ (km)	$y$ (km)	$z$ (km)	$v_x$ (km/s)	$v_y$ (km/s)	$v_z$ (km/s)
SA	-8.66025403	-72,582.4525	-24,285.7489	0.973083288	0	0
SB	0	-72,587.1941	-24,287.3354	0.972733623	0	0
SC	0	-72,577.7109	-24,284.1624	0.973432881	0	0
SH	-2.88675134	-72,585.0433	-24,278.0058	0.973083324	0	0

**Table 4.** Initial coordinates and velocities for phase I.

constellation can be maintained for another six complete orbits. The constellation is propagated with  $J_2$  perturbation at the starting date of June 29, 2009 22:56 (UTCG). The orbit propagation will include only SA and SB because these satellites are considered in the correction of the drift. Figure 7 shows that the satellites in the in-plane motion will maintain the desired benchmark configuration for another 6 complete orbits before the constellation violates the separation distance constraints again. Also, the arrow indicates the time when the first correction is made. The constellation may violate the separation distance constraints earlier because the drift is assumed to be small at the apogee point, but, at least for six complete orbits, the constellation maintains the configuration. Moreover, the active control scheme ensures that the constellation will maintain the configuration at the following apogee point, even though the perturbations are still present when the correction is performed.

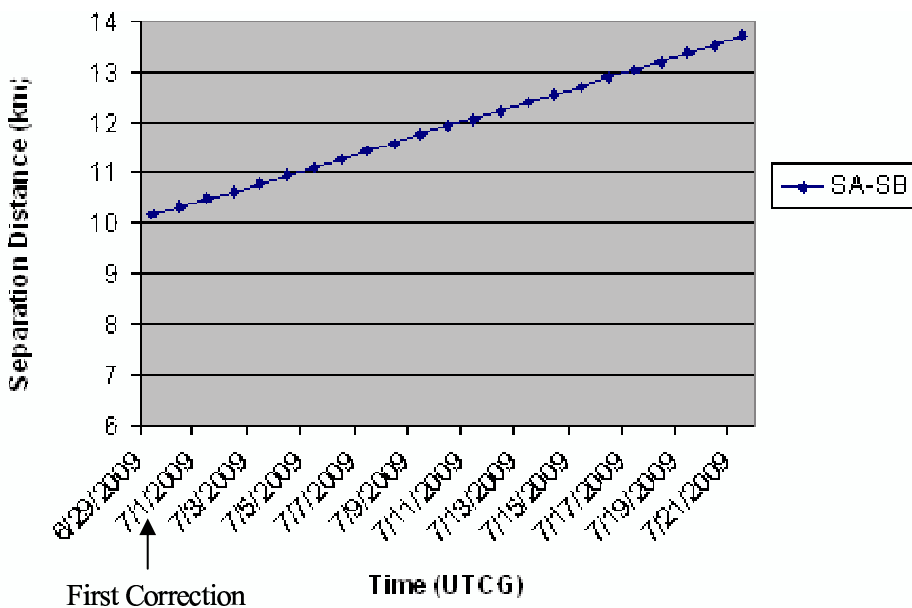


**Figure 7.** Satellite separation for in-plane motion with  $J_2$  perturbation only for phase I.

### 13. Conclusion

The NASA benchmark tetrahedron constellation will not satisfy the separation distance constraints with perturbations, and an active control scheme is needed to maintain the separation distance conditions. To define the motion of a pair of satellites about Earth in an elliptical orbit, the linearized Tschauner–Hempel (TH) equations are used. The linear quadratic regulator (LQR) technique is used as an active control strategy in which two different control schemes are used to maintain the separation distance constraints of the NASA Benchmark tetrahedron constellation depending on the varying term in the TH equations. The Bainum, Strong, and Tan (BST) active control scheme adapts in a piecewise manner the varying term in the TH equations; on the other hand, a different LQR control scheme is defined for the cost function using the Carter–Humi (CH) approach. The CH technique developed a different cost function based on the true anomaly angle and eccentricity of the orbit.

When the simulations to correct the drift for the first specific size (phase I) of the tetrahedron constellation are performed, the LQR control scheme shows a (relative) impulsive type response for both control schemes, but the CH active control scheme shows a lower thrust level than in the BST active control scheme because the CH active control scheme is varying with respect to the true anomaly angle and is explained in terms of the eccentricity. Furthermore, the eccentricity must be part of the equations of motion to obtain a better approximation of the ellipse. [Marec \[1979\]](#) established that for an eccentric orbit, the true anomaly angle must be defined in the cost function to obtain a minimum time and consumption problem. Given these results the LQR using the CH approach gives a lower consumption problem than in the BST control scheme because the BST control scheme keeps constant the varying term for short periods of time.

After the first correction is performed to maintain the separation distance conditions, the simulations show that the pair of satellites analyzed in this paper is going to satisfy the separation distance constraints for at least another 6 complete orbits before the constraints are violated again. For the simulations already presented in this paper, the pair of satellites within the constellation is going to satisfy the separation distance constraints at the next apogee point.

### References

- [Athans and Falb 1966] M. Athans and P. L. Falb, *Optimal control: an introduction to the theory and its applications*, McGraw-Hill, New York, 1966.
- [Bainum et al. 2004] P. M. Bainum, Z. Tan, and X. Duan, “[Review of station keeping strategies for elliptically orbiting constellations in along-track formation](#)”, pp. 350–353 in *Eighth pan american congress of applied mechanics* (Havana, Cuba), vol. 10, January 5–9 2004. also in *International Journal of Solids and Structures*, **42**: 21–22 (October 2005), pp. 5683–5691, PACAM VIII Special Issue.
- [Borse 2000] G. J. Borse, *Numerical methods with MATLAB, a resource for scientists and engineers*, International Thompson Publishing, Boston, 2000.
- [Capó-Lugo 2005] P. A. Capó-Lugo, “Strategies and control schemes to satisfy the separation distance constraints for the NASA benchmark tetrahedron constellation”, Master’s Thesis, Howard University, Washington D. C., December 2005.
- [Capó-Lugo and Bainum 2005a] P. A. Capó-Lugo and P. M. Bainum, “Implementation of the strategy for satisfying distance constraints for the NASA benchmark tetrahedron constellations”, pp. 1463–1482 in *Proceedings of the AAS/AIAA astrodynamics conference* (South Lake Tahoe, CA), edited by B. G. Williams et al., *Advances in the astronomical sciences* **123**, Univelt, San Diego, CA, August 7–11 2005. Paper AAS 05-344.

- [Capó-Lugo and Bainum 2005b] P. A. Capó-Lugo and P. M. Bainum, “Strategy for satisfying distance constraints for the NASA benchmark tetrahedron constellation”, pp. 775–793 in *Proceedings of the 15th annual AAS/AIAA spaceflight mechanics meeting* (Copper Mountain, CO), edited by D. A. Vallado et al., Advances in the astronautical sciences **120**, Univelt, San Diego, CA, January 23–27 2005. Paper AAS 05-153.
- [Carpenter et al. 2003] J. R. Carpenter, J. A. Leitner, and R. D. Folta, David C. and Burns, “Benchmark problems for spacecraft formation flying missions”, in *AIAA guidance, navigation, and control conference and exhibit* (Austin, TX), August 11–14 2003. Paper AIAA-2003-5364.
- [Carter 1990] T. Carter, “New form for the optimal rendezvous equations near a keplerian orbit”, *J. Guid. Control Dynam.* **13**:1 (1990), 183–186.
- [Carter and Brient 1992] T. Carter and J. Brient, “Fuel-optimal rendezvous for linearized equations of motion”, *J. Guid. Control Dynam.* **15**:6 (1992), 1411–1416.
- [Carter and Humi 1987] T. Carter and M. Humi, “Fuel-optimal rendezvous near a point in general keplerian orbit”, *J. Guid. Control Dynam.* **10**:6 (1987), 567–573.
- [Gerald and Wheatley 2004] C. F. Gerald and P. O. Wheatley, *Applied numerical analysis*, 7th ed., Addison-Wesley, New York, 2004.
- [Marec 1979] J. P. Marec, *Optimal space trajectories*, vol. 1, Studies in astronautics, Elsevier Scientific, Amsterdam, 1979.
- [Massari et al. 2004] M. Massari, R. Armellin, and A. E. Finzi, “Optimal trajectory generation and control for reconfiguration maneuvers of formation flying using low-thrust propulsion”, pp. 2461–2474 in *Proceedings of the 14th annual AAS/AIAA spaceflight mechanics meeting* (Maui, Hawaii), edited by S. L. Coffey et al., Advances in the astronautical sciences **119**, Univelt, San Diego, CA, February 8–12 2004. Paper AAS 04-258.
- [Mishne 2004] D. Mishne, “Controlling the out-of-plane motion of a follower satellite in a periodical relative trajectory, using angular rate information”, in *AIAA/AAS astrodynamics specialist conference and exhibit* (Providence, RI), August 16–19 2004. Paper AIAA 2004-5215.
- [Phillips and Nagle 1995] C. L. Phillips and H. T. Nagle, *Digital control system analysis and design*, 3rd ed., Prentice Hall, Englewood Cliffs, NJ, 1995.
- [STK 2003] *STK, Satellite Tool Kit Software*, Analytical Graphics, Inc., Malvern, PA, 2003. Version 5.0.
- [Strang 1986] G. Strang, *Introduction to applied mathematics*, Wellesley-Cambridge Press, Wellesley, Mass., 1986.
- [Strong 2000] A. Strong, *On the deployment and station keeping dynamics of n-body orbiting satellite constellations*, Ph.D. Dissertation, Howard University, Washington D. C., 2000.
- [Tan et al. 1999] Z. Tan, P. M. Bainum, and A. Strong, “A strategy for maintaining distance between satellites in an orbiting constellation”, pp. 343–354 in *Proceedings of the 9th Annual AAS/AIAA space flight mechanics meeting* (Breckenridge, CO), edited by R. H. Bishop et al., Advances in the astronautical sciences **102**, Univelt, San Diego, CA, February 7–10 1999. Paper AAS 99-125.
- [Tan et al. 2002] Z. Tan, P. M. Bainum, and A. Strong, “The implementation of maintaining constant distance between satellites in coplanar elliptic orbits”, *J. Astronaut. Sci.* **50**:1 (2002), 53–69.

Received 16 May 2006. Accepted 20 Apr 2007.

PEDRO A. CAPÓ-LUGO: [pcapo@howard.edu](mailto:pcapo@howard.edu)

Department of Mechanical Engineering, Howard University, 2300 Sixth Street NW, Washington, DC 20059, United States

PETER M. BAINUM: [pbainum@fac.howard.edu](mailto:pbainum@fac.howard.edu)

Department of Mechanical Engineering, Howard University, 2300 Sixth Street NW, Washington, DC 20059, United States